J Ornithol (2017) 158:761–772
DOI 10.1007/s10336-017-1448-5

ORIGINAL ARTICLE

Genetic structure and population history of wintering Asian Great Bustard (*Otis tarda dybowskii*) in China: implications for conservation

Gang Liu[1] · Xiaolong Hu[2] · Aaron B. A. Shafer[3] · Minghao Gong[1] · Morigen Han[4] · Changjiang Yu[4] · Jingying Zhou[4] · Jie Bai[4] · Derong Meng[5] · Guohai Yu[6] · Dapeng Dang[7]

Received: 27 September 2016 / Revised: 11 February 2017 / Accepted: 1 March 2017 / Published online: 14 March 2017

Abstract Wintering areas affect population processes and genetic structuring of many bird species. The Asian Great Bustard (*Otis tarda dybowskii*) is declining across its range as its breeding and wintering grounds become more fragmented. No genetic information for this vulnerable subspecies in the wild exists. We used noninvasive fecal sampling and mitochondrial sequencing to quantify the level of genetic diversity and the extent of genetic differentiation within and among the wintering populations. Bayesian skyline plot (BSP) analysis was conducted to assess changes in population size over the last several thousand years. Overall, 17 haplotypes were identified in 101 individuals from six wintering grounds, with mean haplotype diversity of 0.90 ± 0.02. Significant population differentiation among wintering grounds was observed [population pairwise test (Φ_{ST}) = 0.13, $p < 0.001$], with genetic differentiation associated with geographical distance ($R^2 = 0.26$, $p < 0.05$) and pairwise tests consistent with some degree of population admixture. The BSP exhibited a gradual increase in effective population size beginning around 28,000 years ago, but a decrease starting approximately 4000 years ago. Given that China has the most important wintering grounds for the Asian Great Bustard, and that these are becoming increasingly fragmented, it is likely necessary to establish more protected areas to facilitate the protection and monitoring of wintering Great Bustards.

Keywords Demography · Admixture · Great Bustard · Population differentiation · Genetic differentiation · Bayesian skyline plot

Communicated by M. Wink.

G. Liu and X. Hu contributed equally to this work.

Electronic supplementary material The online version of this article (doi:10.1007/s10336-017-1448-5) contains supplementary material, which is available to authorized users.

✉ Minghao Gong
gongmh2005@hotmail.com

[1] Research Institute of Wetland, Beijing Key Laboratory of Wetland Services and Restoration, Chinese Academy of Forestry, Beijing 100091, China

[2] Laboratory of Non-invasive Research Technology for Endangered Species, College of Nature Conservation, Beijing Forestry University, Beijing 100083, China

[3] Forensic Science, Environmental and Life Sciences, Trent University, Peterborough 7K9J 7B8, Canada

[4] Tumuji National Nature Reserve, 137600 Zhalaite, Inner Mongolia Autonomous Region, China

[5] Biology Department, Cangzhou Normal College, Cangzhou 061001, Hebei, China

[6] Momoge National Nature Reserve, Baichen 137316, Jilin, China

[7] Yellow River Wetland Protection and Management Station, Dali 715100, Shaanxi, China

Zusammenfassung

Genetische Struktur und Populationsgeschichte überwinternder asiatischer Großtrappen (*Otis tarda dybowskii*) in China: Implikationen für ihren Schutz

Wintergebiete beeinflussen Populationsprozesse und die genetische Strukturierung vieler Vogelarten. Die asiatische Großtrappe (*Otis tarda dybowskii*) ist durch zunehmende Fragmentierung ihrer Lebensräume im Brut- wie Überwinterungsgebiet in ihren Beständen rückläufig. Bisher gibt es keine genetische Information

für diese „verwundbare“Unterart von freilebenden Vögeln. Mittels Sequenzierung mitochondrialer DNA aus Kotproben quantifizierten wir die genetische Vielfalt und das Ausmaß der genetischen Differenzierung innerhalb und zwischen überwinternden Populationen. Wir führten eine Bayesische Skyline Plot (BSP)-Analyse durch, um Veränderungen in der Populationsgröße in den vergangenen Jahrtausende zu beurteilen. Insgesamt wurden 17 Haplotypen von 101 Individuen aus 6 Wintergebieten mit einer mittleren Haplotypenvielfalt von 0.90 ± 0.02 identifiziert. Die verschiedenen Überwinterungspopulationen waren signifikant verschieden ($\Phi_{ST} = 0.13$, $p < 0001$), wobei die genetische Differenzierung mit dem geographischen Abstand ($R^2 = 0.26$, $p < 0.05$) verbunden ist, und paarweise Tests zeigen, dass eine gewissen Durchmischung der Populationen besteht. Die BSP ergab eine allmähliche Zunahme der effektiven Populationsgröße beginnend vor etwa 28.000 Jahren bis etwa 4000 Jahren vor heute. Seither nehmen die Bestände ab. Angesichts der Tatsache, dass in China die wichtigsten Überwinterungsgebiete für die asiatische Großtrappe liegen, die aber zunehmend fragmentiert werden, ist die Einrichtung weitere Schutzgebiete anzustreben, um den Schutz der Großtrappe aber auch das Monitoring der Winterbestände zu erleichtern.

Introduction

In response to variable environments across space and time, birds select different and often widely distributed wintering sites to gain access to limited resources (Piper 2011; van Wijk et al. 2016). Avian wintering habitats have generally decreased and become more concentrated because of severe human disturbance, decreased food availability and global climate change, which subsequently can cause declines of population size (Maclean et al. 2006) and behavioral (i.e., differential migration) and physiological responses [i.e., corticosterone stress (Holberton and Able 2011)]. Many Holarctic species will summer in the same general area, but migrate to different winter ranges; in such instances genetic analyses have revealed panmixia, ring species divergence and population subdivision among differing wintering groups (Bensch et al. 2009; Lee et al. 2010; von Rönn et al. 2016). A multitude of genetic structuring scenarios combined with growing evidence for limited natal philopatry (Weatherhead and Forbes 1994) and the effect of winter habitat on population processes (Studds and Marra 2005) suggest that wintering areas are of paramount importance for many species.

The Great Bustard (*Otis tarda*) is a globally threatened species, listed as vulnerable worldwide under the current International Union for Conservation of Nature criteria (BirdLife International 2012). There are two recognized subspecies, the nominal (*Otis tarda tarda*) and Asian Great Bustard (*Otis tarda dybowskii*), that are geographically isolated and differ significantly in population size. The population size of the nominal subspecies is estimated to be 50,000, mainly distributed in Spain and mainland Europe (Alonso 2010; Palacín and Alonso 2008); the Asian subspecies is estimated to have between 1500 and 2200 individuals across its range of Russian South Siberia, Mongolia and China (Mi et al. 2016). While the overall population of the nominal Great Bustard is considered stable, due to agricultural intensification, habitat degradation and illegal hunting, the population of the Asian Great Bustard has been declining in China (Alonso 2010).

The Asian Great Bustard was widely distributed across China before 1900. By the end of the twentieth century its distribution had decreased and its populations had become isolated due to the loss and fragmentation of breeding and wintering habitat (BirdLife International 2001; Jiang 2004). According to the first national terrestrial wildlife survey in China (State Forestry Administration 2001), the wintering grounds of the Great Bustard have contracted to three regions: the middle and lower reaches of the Yellow River (an estimated 303 wintering individuals), the middle and lower reaches of the Yangtze River (an estimated 168 wintering individuals), and the Songnen Plain of northeast China [an estimated 145 wintering individuals (Jiang 2004; see Fig. 1)]. In the last decade, only a fraction of Great Bustards have been observed wintering in the middle and lower reaches of the Yangtze River, apparently due to a lack of suitable wintering habitats (State Forestry Administration 2016). There is growing concern that the remaining wintering grounds will continue to be eroded unless urgent conservation measures are taken. The Asian Great Bustard is also a long-distance migratory bird, with a migration route twice as long as that reported for its counterpart, the nominal Great Bustard (Kessler et al. 2013). Because the Asian Great Bustard spends two-thirds of the year at migratory stopover sites and wintering grounds it faces various threats in the migratory period due to its use of human-dominated landscapes (Di and Du 2016). Interestingly, evidence of partial migration, i.e., the stopping of migration by some individuals, has recently been reported (Li et al. 2005; Qiao et al. 2008; Yu 2015).

Under the Asian Great Bustard's current discontinuous and fragmented distribution, combined with changes of migratory patterns, identifying geographically restricted genetic lineages under threat is paramount to conservation efforts. Genetic information is non-existent for the wild populations of Asian Great Bustard, largely due to the difficulty and species sensitivity to sampling (e.g., Anna et al. 2008). Further, the classification of *O. tarda tarda* and *O.*

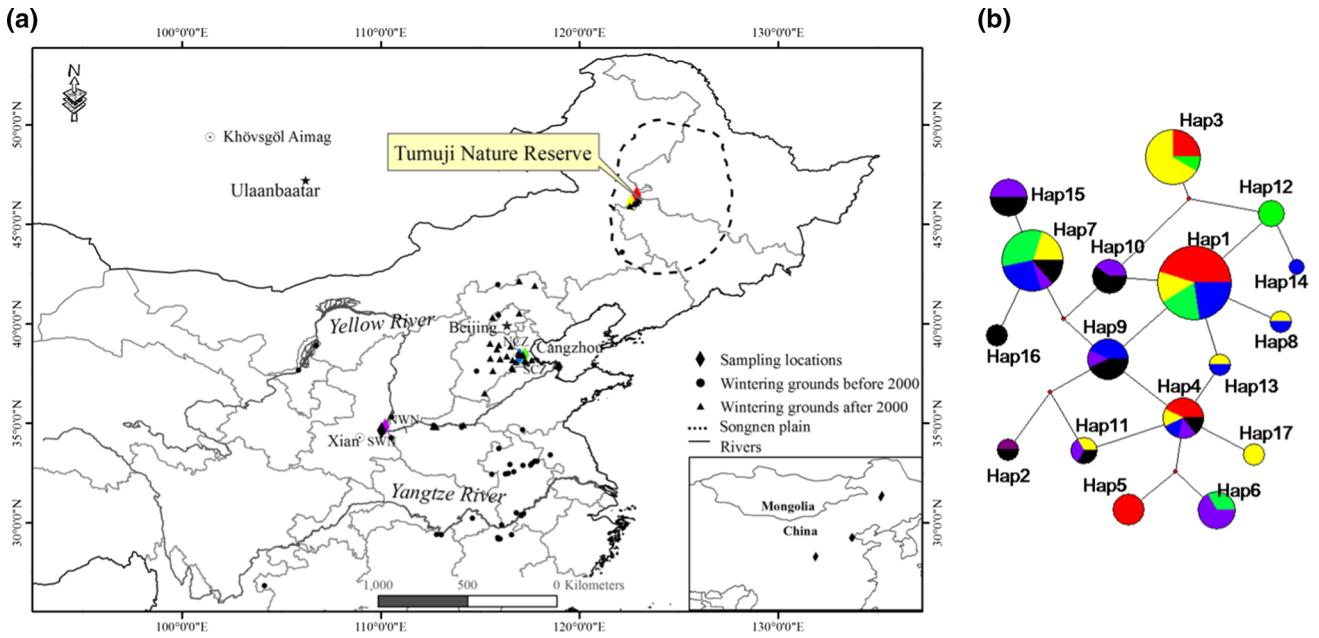

Fig. 1a, b Study region and median-joining haplotype networks. **a** Sampling localities of Asian Great Bustard (*Otis tarda dybowskii*) across its wintering distribution range in China. *Diamonds* represent samples from the wintering grounds, *circles* represent the occurrence of Great Bustards in wintering grounds from the 1960s to 2000, *triangles* represent the occurrence of Great Bustards in wintering grounds from 2000 to the present, *dashed circle* represents the Songnen Plain. **b** Unrooted median-joining network based on 332-base pair sequences of the mitochondrial DNA (mtDNA) control region for 101 individuals from six wintering populations of Asian Great Bustard. Haplotype sizes are proportional to their observed frequencies (see Table 2). *Red* Kaoshan, *yellow* Maanshan, *green* northern Cangzhou, *blue* southern Cangzhou, *purple* northern Weinan, *black* southern Weinan (color figure online)

tarda dybowskii as distinct subspecies is based primarily on geopolitical criteria (http://avibase.bsc-eoc.org). The effective prioritization for conservation to save declining species depends heavily on taxonomic decisions, and the policy decisions can be delayed or deferred if the taxonomic status in question is uncertain (Gamauf et al. 2005; Torstrom et al. 2014). As an important step in accurately and efficiently deploying conservation efforts and resources, population and subspecies boundaries should be defined and clarified (Idaghdour et al. 2004). In this study we used noninvasive fecal sampling of Asian Great Bustard across their wintering grounds in China to quantify the genetic diversity and investigate the extent of genetic differentiation within and among the wintering populations. Bayesian skyline plot (BSP) analysis was conducted to assess changes in population size over the last several thousand years, and we examined phylogenetic relationships between the closely related taxa (*O. tarda tarda* and *O. tarda dybowskii*).

Materials and methods

Samples

Fecal sampling was conducted from December 2015 to March 2016 at six locations separated into three geographical regions (Fig. 1). Fecal samples ($n = 120$) were collected at six wintering grounds, specifically, 22 from the Kaoshan core area of Tumuji Nature Reserve in Inner Mongolia (KS; 46°29′N, 122°52′E), 23 from Maanshan military forbidden area in Jilin province (MAS; 46°03′N, 122°36′E), 18 from northern Cangzhou in Hebei province (NCZ; 38°25′N, 117°16′E), 19 from southern Cangzhou in Hebei province (SCZ; 38°22′N, 117°0′E), 20 from northern Weinan in Shaanxi province (NWN; 34°50′N, 110°13′E,), and 18 from the southern Weinan in Shaanxi province (SWN; 34°38′N, 110°03′E) (Fig. 1). The overnight roosts and foraging grounds of the Great Bustard were observed with telescopes and, once birds flew away, fresh fecal samples were collected immediately. To minimize the probability of re-collecting fecal samples from the same individual, we selected the sampling location where no old feces were left and only fresh feces were collected. Samples at each sampling location were collected only once, with a minimum distance of 2 m between samples. All fecal samples were stored in a cooler during sample collection, then preserved at −20 °C in a freezer.

DNA extraction, polymerase chain reaction and sequencing

DNA from fecal samples was extracted using the QIAamp DNA Stool Mini Kit (QIAGEN, Germany). The fecal DNA was amplified at the 5′ end partial sequence of the

mitochondrial DNA (mtDNA) control region, using primers 5′-CTAACCTATGTATAACTGTGC-3′ and 5′- GG AAAGAATGGGCCTGAAGCTAGT-3′ designed using Primer Premier 6 based on the complete mitochondrial genome of *O. tarda tarda* (Genbank accession no. FJ751803). The targeted polymerase chain reaction (PCR) fragment size is 452 base pairs (bp). PCR reactions were performed in a total volume of 25 μL containing 2 × Taq PCR MasterMix (Biomed, China), 2 μL template DNA, 0.5 μM of each primer, 12.5 μL H_2O and 0.05 μL BSA (10 mg/mL; Takara). PCR amplifications were carried out using an initial denaturation step at 95 °C for 5 min, followed by 30 cycles of 95 °C for 1 min, 55.6 °C for 1 min, and 72 °C for 2 min, and a final extension at 72 °C for 10 min. Negative controls were used in the whole process of DNA extraction and PCR. PCR products were detected by 1.5% agarose gel electrophoresis. If the target band was confirmed, PCR products were purified using QIAquick PCR purification kits (QIAGEN). Sequence reactions were performed for both DNA strands by using the ABI BigDyeTM Terminator Cycle Sequencing Kit, and the products were electrophorized on an ABI Prism3100 sequencer DNA sequencer (PE Applied Biosystems). The same primers as above were used for sequencing.

Genetic diversity and population structure analyses

The sequences were aligned with Mega 5.0 (Tamura et al. 2011) and the alignments manually verified. The number of haplotypes (h), haplotype diversity (H_d), and nucleotide diversity (π) were calculated for all populations using DnaSP version 5 (Librado and Rozas 2009). Analyses of molecular variance (AMOVA) implemented in Arlequin 3.5 (Excoffier and Lischer 2010) were performed to assess the proportion of genetic variance within and among wintering grounds. Based on the Tamura–Nei model [as Hasegawa–Kishino–Yano (HKY) is not implemented in this analysis], genetic distance (population pairwise test; Φ_{ST}) was calculated and significance was assessed from 10,000 permutations. Significance levels were adjusted for multiple testing using the sequential Bonferroni procedure (Rice 1989). We tested for an association between $\Phi_{ST}/(1 - \Phi_{ST})$ and the logarithm of geographical distance in kilometers using a Mantel test implemented in IBD 1.1 (Bohonak 2002) with 10,000 permutations. To visually inspect genetic differentiation among regions of genetically related populations, we performed a multidimensional scaling (MDS) analysis with estimates of Φ_{ST} from all possible pairwise comparisons of populations as a dissimilarity measure using PRIMER version 7 (Clarke and Gorley 2015).

Phylogenetic analyses

We constructed unrooted haplotype networks using the median-joining algorithm to depict the relationships among haplotypes from different wintering populations (Bandelt et al. 1999), which was implemented in Network version 4.516 (http://www.fluxus-engineering.com). Phylogenetic trees of the wintering Asian Great Bustards were constructed to assess control region sequence distribution using Bayesian inference in MrBayes version 3.1.2 (Ronquist and Huelsenbeck 2003). The HKY model was selected as the best-fitting nucleotide substitution model using the Akaike information criterion in jModelTest version 2 (Darriba et al. 2012). Four independent runs with default heating temperatures were run for two million steps and sampled every 1000th step. The first 25% of samples were discarded as burn-in. Convergence of the Markov chain Monte Carlo (MCMC) chains was assessed using Tracer version 1.6 (Rambaut et al. 2014). The phylogenetic tree was rooted using a homologous sequence from the nominal Great Bustard subspecies (*O. tarda tarda*; GenBank accession no. DQ445305).

In order to assess the taxonomic status of the Asian Bustards, phylogenetic trees were constructed using available control region sequences of Great Bustard and Houbara Bustard. Both Bayesian inference and maximum parsimony (MP) methods were used for phylogenetic construction. The Bayesian analyses were performed using MrBayes version 3.1.2 (Ronquist and Huelsenbeck 2003). Markov chains were run for 20 million generations, and trees were sampled every 1000 generations. Tracer version 1.6 was used to confirm when the log likelihood of sampled trees reached stationarity, and the remaining samples were used to generate the consensus tree and the Bayesian posterior probability (BPP). MP analyses were conducted using PAUP 4a (Swofford 2003). For nodal support assessment, a nonparametric bootstrap with 1000 replicates was used. BPPs greater than 0.95 and BSPs greater than 70% were considered strong support (Erixon et al. 2003). The timing of divergence between *O. tarda dybowskii* and *O. tarda tarda* was estimated in ARLEQUIN as the corrected pairwise sequence distance between species minus the corrected pairwise sequence distance within a species, which we here refer to as the corrected sequence divergence (d_{corr}) (Tamura and Nei 1993). Because no fossil record was available, we assumed a range of substitution rate (1–1.5%/10^6 years per lineage) for the control region fragment (Horreo et al. 2013).

Population demographic history

Two different approaches were applied to elucidate historical demographic events (i.e., recent expansions,

Table 1 Genetic diversity indices, neutrality tests and mismatch distribution results for wintering populations and geographical wintering regions of the Asian Great Bustard

Population	*n*	*S*	*h*	H_d (SD)	π (SD)	*D*	F_S	SSD	*r*
KS	20	7	4	0.70 (0.08)	0.007 (0.001)	0.78	2.42	0.06	0.18
MAS	20	9	8	0.82 (0.07)	0.009 (0.001)	0.74	−0.76	0.05*	0.10
NCZ	15	8	5	0.81 (0.06)	0.008 (0.001)	0.54	1.11	0.05	0.09
SCZ	16	7	7	0.84 (0.06)	0.006 (0.001)	−0.28	−1.81	0.01	0.04
NWN	15	9	8	0.90 (0.05)	0.010 (0.001)	0.69	−1.42	0.02	0.06
SWN	15	8	7	0.89 (0.04)	0.007 (0.001)	−0.01	−1.27	0.02	0.10
Region 1	40	10	9	0.81 (0.04)	0.009 (0.002)	0.72	−0.17	0.04	0.09
Region 2	31	9	10	0.83 (0.04)	0.008 (0.001)	0.12	−2.37	0.01	0.03
Region 3	30	10	9	0.90 (0.02)	0.008 (0.001)	0.59	−0.69	0.01	0.06
Total	101	13	17	0.90 (0.02)	0.009 (0.000)	0.49	−3.50*	0.03	0.10

N Number of individuals, *S* number of polymorphic sites, *h* number of haplotypes, H_d haplotype diversity, π nucleotide diversity, *D* Tajima's *D*, F_S Fu's F_S, *SSD* sum of squares deviation, *r* Harpending's raggedness index, *KS* Kaoshan, *MAS* Maanshan, *NCZ* northern Cangzhou, *SCZ* southern Cangzhou, *NWN* northern Weinan, *SWN* southern Weinan

* $p < 0.05$

declines, selection). We first used neutrality tests on the data in a hierarchical manner (wintering ground, region, entire data set). Tajima's *D* (Tajima 1989) and Fu's F_S (1997) tests based on the difference between two alternative estimates of the mutational parameter (θ), were estimated in DnaSP (Librado and Rozas 2009). We also conducted mismatch distribution analyses (Rogers and Harpending 1992) in ARLEQUIN. Here, unimodal curves and non-significant values of the raggedness index (*r*) indicate that populations have not deviated from the expected model of rapid expansion (Harpending 1994).

Second, the population history of the Asian Great Bustards was investigated by using the BSP (Heled and Drummond 2008). The BSP model generates a posterior distribution of effective population size through time using MCMC sampling. The MCMC analysis was run for 3×10^7 generations (sampled every 1000 iterations), of which the first 10% was discarded as burn-in. The substitution model used was informed by prior runs in jModelTest (see above). We assumed a Bayesian skyline tree prior and a piecewise-constant skyline model (with a random starting tree). The mtDNA control region mutation rate is not known for Asian Great Bustards, so we used a mutation rate consistent with previous work on the nominal subspecies [$\mu = 1 \times 10^{-7}$/site per year (Horreo et al. 2013)]. We conducted two independent MCMC runs to ensure convergence and congruent effective sample sizes (>200). Results were visualized and checked using Tracer version 1.6 (Rambaut et al. 2014). The effective population size (N_e) was calculated from the range of substitution rates and θ derived from the mismatch distribution analysis with the formula $\theta = 2N_e\mu$ (Tajima 1989), where N_e is the effective female population size. The range of substitution rates is 0.10–0.15 substitutions/site per 10^6 years, where the generation time of the Great Bustard is estimated at 8.69 years (Horreo et al. 2013).

Results

Sampling and PCR success

A total of 101 samples yielded successful DNA extractions and sequencing results (Table S1). PCR success rate in KS, MAS, NCZ, SCA, NSX, SSX was 90.91, 86.96, 83.33, 84.21, 75.00, 83.3%, respectively, with an average of 83.95 ± 5.26%. The differences in PCR success rate among three sampling populations were not significant ($\chi^2 = 0.67$, $p > 0.05$). To maximize the sample number as some samples yielded shorter reliable sequences, we analyzed 332 bp of the control region that was present in all 101 samples.

Genetic diversity

The genetic diversity indices for partial mtDNA control region sequences showed moderate levels of genetic variation in Asian Great Bustards (Table 1). We detected 13 variable sites and no indels. A total of 17 haplotypes were observed in the 101 individuals across the six wintering grounds (GenBank accession nos. KX685501–KX685513, KX767084–KX767087), with haplotype diversity ranging from $h = 0.70$ to 0.90 (Table 1). Among the haplotypes, only one (Hap14) was observed in a single individual (in the SCZ population) and many were shared across populations (Table 2).

Table 2 Variable sites and geographic distribution of mitochondrial DNA (mtDNA) control region haplotypes (*HAP*) in six populations of the Asian Great Bustard; for other abbreviations, see Table 1

Haplotype	Variable positions													Individuals per wintering population						Total
	16,502	16,514	11,515	16,544	16,565	16,582	16,587	16,593	16,594	16,643	16,648	16,653	16,680	KS	MAS	NCA	SCZ	NWN	SWN	
Hap1	G	C	T	A	C	A	T	G	T	G	A	G	T	10	3	4	5			22
Hap2	A	.	.	.	.	.	.	.	.	A	.	A	.					1	1	2
Hap3	.	T	C	.	.	G	.	.	.	.	.	.	.	3	8	1				12
Hap4	.	.	.	.	.	.	C	.	.	.	.	A	.	3	1		1	1	1	7
Hap5	.	.	.	.	T	.	C	.	.	A	.	A	.		4					4
Hap6	.	.	.	.	T	.	C	.	.	.	G	A	.			2		4		6
Hap7	.	.	C	.	.	.	.	.	C	.	.	A	.		3	5	4	1	2	15
Hap8	.	.	.	.	T	.	.	.	.	.	.	.	.		1		1			2
Hap9	.	.	.	.	.	.	.	.	.	.	.	A	.				3	1	3	7
Hap10	.	.	C	.	.	.	.	.	.	.	.	.	.					2	3	5
Hap11	A	.	.	.	.	.	C	.	.	.	.	A	.			1		1	1	3
Hap12	.	.	.	.	.	G	.	.	.	.	.	.	.			3				3
Hap13	.	.	.	.	.	.	C	.	.	.	.	.	.		1		1			2
Hap14	.	.	.	.	.	G	.	.	.	A	.	.	.				1			1
Hap15	.	.	C	.	.	.	.	A	C	.	.	A	.					3	3	6
Hap16	.	.	C	G	.	.	.	.	C	.	.	A	.						2	2
Hap17	.	T	.	.	.	.	C	.	.	.	.	A	C		2					2

Table 3 Hierarchical analysis of molecular variance based on mtDNA control region of the Asian Great Bustard

Source of variation	*df*	Sum of squares	Variance components	Percentage of variation	*F*-statistics
Among regions	2	12.45	0.10	6.61	$F_{CT} = 0.07$
Among populations within regions	3	8.59	0.09	5.95	$F_{ST} = 0.13$*
Within populations	95	126.88	1.34	87.44	$F_{SC} = 0.06$
Total	100	147.92	1.53		

* $p < 0.01$

Table 4 Pairwise estimates of F_{ST} between wintering populations of the Asian Great Bustard in China; for abbreviations, see Table 1

	KS	MAS	NCZ	SCZ	NWN	SWN
KS	–					
MAS	0.10	–				
NCZ	0.06	0.05	–			
SCZ	0.04	0.13*	-0.02	–		
NWN	0.14*	0.19*	0.07	0.10	–	
SWN	0.25*	0.19*	0.07	0.10*	0.08	–

* $p < 0.05$

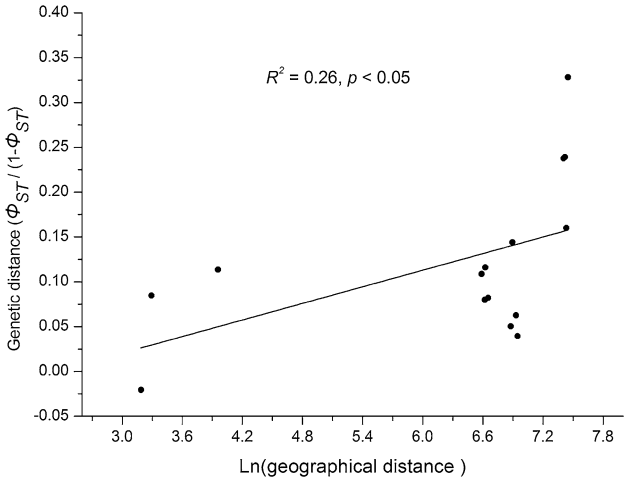

Fig. 2 Isolation-by-distance pattern for Asian Great Bustard populations in China. *Each point* represents genetic distance [Φ_{ST}/(1 − Φ_{ST})] plotted against log-transformed geographic distance

Population structure and phylogenetic history

The hierarchical AMOVA revealed that 87.44% of the total genetic variation was partitioned within populations, with 5.95% ($p < 0.001$) among populations (Table 3). An estimated 6.61% of the variation was distributed among geographical regions ($F_{CT} = 0.07$, $p > 0.05$; Table 3). Genetic differentiation among the six wintering populations had a global Φ_{ST} of 0.13 ($p < 0.05$; Table 3). Multiple population pairwise tests (Φ_{ST}) revealed that mtDNA haplotype frequencies were significantly different in six out of 15 comparisons (Table 4). The highest genetic distance was observed for the KS population in comparison to the SWN population ($\Phi_{ST} = 0.25$, $p < 0.01$), while the lowest and non-significant level of differentiation was between the NCZ and the SCZ population (Table 4). No significant genetic differentiation between populations within one region was observed ($\Phi_{SC} = 0.06$, $p > 0.05$; Table 3).

The haplotype median-joining network showed a star-like topology with no clear geographic structures (Fig. 1). The network was concordant with the Bayesian tree that was marked by shallow sequence divergence and no well-supported basal clades (Fig. S1). The MDS analysis based on Φ_{ST} values as a dissimilarity measure revealed no clear geographical structure among individuals from wintering grounds. The stress value for the two-dimensional representation was 0.03 suggesting high reliability of the MDS analysis (stress value < 0.05; Fig. S2). Tests for IBD across these wintering grounds showed an effect of geographic distance, although this was likely driven by a few data points ($R^2 = 0.26$, $p < 0.05$; Fig. 2).

The Bayesian and MP analyses produced nearly identical trees (only the Bayesian tree is presented; Fig. 3). *O. tarda and Chlamydotis undulata* formed a well-demarcated clade with high bootstrap values of 94% and BPP = 1. Furthermore, haplotypes of *O. tarda tarda* and *O. tarda dybowskii* formed two separate subclades (BPP = 0.98, BSP = 95%), while *Chlamydotis undulata fuertaventurae* and *Chlamydotis undulata undulata* clustered together. There were substantial differences between the subclades but relatively few differences among haplotypes within each subclade (Table 5). Sequence divergence between *O. tarda dybowskii* and *O. tarda tarda* haplotypes ($d_{corr} = 0.025$) suggests that the divergence occurred in the Early Pleistocene between 1.67 and 2.50 million years ago. All estimates had relatively large confidence intervals because we used a range of mutation rates to calibrate the molecular clock (Horreo et al. 2013).

Population history

Neither Tajima's *D* or Fu's F_S showed significant deviations from null expectations of selective neutrality for

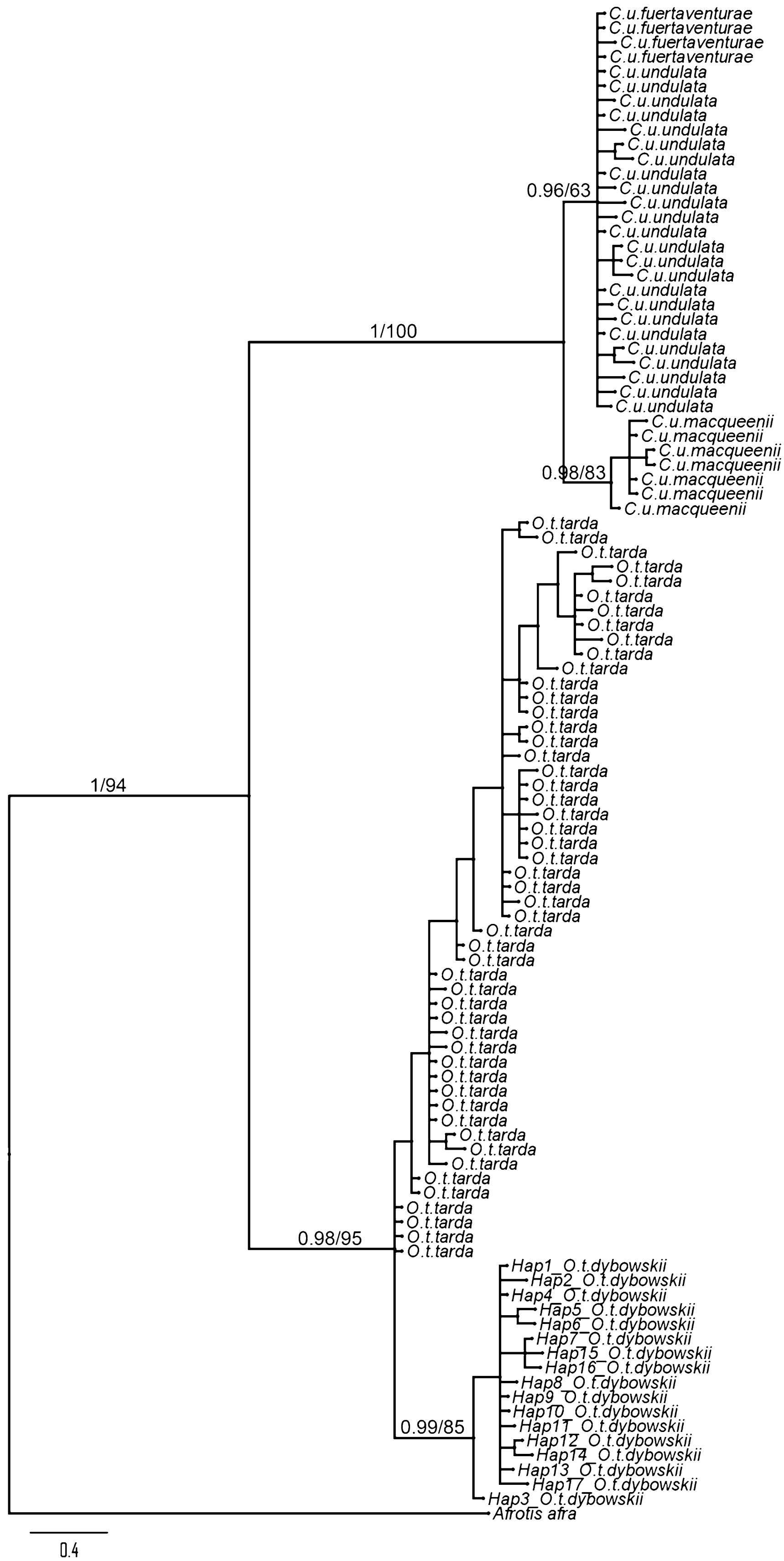

Fig. 3 Phylogenetic tree of the mitochondrial control region haplotypes inferred from a Bayesian analysis. *Numbers above* or *beside nodes* are Bayesian posterior probabilities (BPPs) and maximum likelihood bootstrap proportions (BSPs) in the format of BPP/BSP. The outgroup is *Afrotis afra* (Genbank accession no. AF328840). Sequences in this tree include the following: the 17 haplotypes identified in *O. tarda dybowskii* in the present study; 35 sequences of three Houbara subspecies [four *Chlamydotis undulata fuertaventurae* (AJ544565-AJ544568), seven *Chlamydotis undulata macqueenii* (AJ544569-AJ544575), 24 *Chlamydotis undulata undulata* (AJ544541-AJ544564)], and 53 sequences of *O. tarda tarda* (AF537990-AF538022, EU232174-EU232175, DQ445296-DQ445305, AF422092-AF422093, AF422095-AF422100, AF422104, AF422106)

Table 5 The corrected pairwise sequence distance between species (*below the diagonal*); SE estimates are shown *above the diagonal*, and corrected pairwise sequence distance within a species *on the diagonal*

	O. tarda dybowskii	*O. tarda tarda*	*Chlamydotis undulata fuertaventurae*	*Chlamydotis undulata macqueenii*	*Chlamydotis undulata undulata*
O. tarda dybowskii	0.010	0.012	0.029	0.029	0.028
O. tarda tarda	0.048	0.013	0.029	0.028	0.029
C. undulata fuertaventurae	0.176	0.175	0.005	0.009	0.003
C. undulata macqueenii	0.177	0.164	0.026	0.003	0.008
C. undulata undulata	0.173	0.171	0.007	0.025	0.009

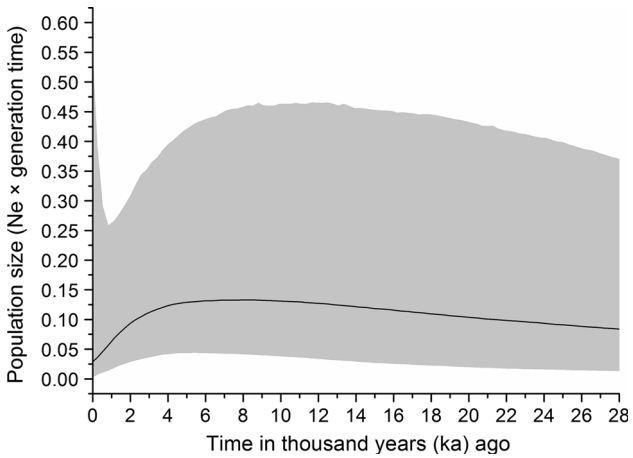

Fig. 4 Bayesian skyline plots (BSPs) for a mutation rate of 1.0×10^{-7}/site per year of the Asian Great Bustard. Population size is the product of the effective size and generation time. *Solid lines* represent median BSP plot values, with the 95% highest probablity density interval shown in *gray*. The *y*-axis values are scaled by mutation rate

either wintering populations or region (Table 1). However, Fu's F_S-test, which has been devised specifically to detect population expansion, showed a significant negative value for the whole dataset ($F_S = -3.50$; $p < 0.05$). The mismatch distribution revealed a smooth and unimodal curve, which was consistent with historical population growth (Fig. S3). The non-significant Harpending's $r = 0.10$ ($p = 0.07$) suggested a good fit of the empirical data to a sudden expansion model for the total sample. The BSP, albeit with wide confidence intervals, exhibited a gradual increase in population size beginning at around 28,000 years before present (BP), but a recent decrease beginning around 4000 BP (Fig. 4). The θ estimated from the best-fit model for the mismatch distribution was 0.00114, and the N_e value ranged from 437 to 656 (Fig. S4).

Discussion

Fecal DNA as a tool for Great Bustard conservation

Molecular scatology has facilitated the study of genetic diversity in endangered species. We present the first large-scale study to quantify genetic variability of the vulnerable Asian Great Bustard. We observed a moderate level of mtDNA genetic diversity across sampling areas ($h = 17$, $H_d = 0.90$, $\pi = 0.009$), which is greater than that previously described for this subspecies in 47 captive individuals (Liu 2006). By comparing the corrected pairwise sequence distance within a species based on the same fragments (309 bp), the Asian Great Bustard showed lower levels of nucleotide diversity than its conspecific the nominal Great Bustard, but higher than any Houbara Bustard subspecies (Table 5). Based on the corrected *p*-distance of 0.048 ± 0.012,our analyses support the subspecies status of *O. tarda dybowskii*, based on the >0.06 threshold often used (Torstrom et al. 2014) and the fact that no nuclear markers were examined. Great Bustards, regardless of their taxonomic status, are facing different threats and clearly require different management strategies in order to secure their persistence (Broders et al. 2003).

The migratory routes and breeding grounds selected by migratory birds will influence the haplotype distribution and frequency of a species (Kraus et al. 2016; Rolshausen et al. 2013). Breeding populations in KS and MAS have recently become sedentary as a result of conservation strategies initiated by Tumuji Nature Reserve, which includes artificial feeding, increased protection from poaching, and prohibited grazing (Li et al. 2005; Yu 2015), and a changing climate (Mi et al. 2016). This migratory switch might have contributed to the genetic structure observed in these two populations (see also Lundberg 2013; Wilson et al. 2011). In addition, the declines of population size, habitat fragmentation, human interference

and a contracted wintering area can result in population differentiation (Kekkonen et al. 2011; Pitra et al. 2011).

Although significant population differentiation was detected for several wintering populations, the median-joining haplotype network and Bayesian phylogeny showed minimal grouping by geography, suggesting wintering admixture exists among populations (Table 4). Moreover, the IBD plots support this (Fig. 2). The mixing of distinct breeding populations in wintering grounds, or individuals of the same breeding population migrating to different places in winter, is a common phenomenon in birds, especially for long-distance migratory species (Chabot et al. 2012; Liu et al. 2012). For example, two rescued Bustards fitted with global positioning system transmitters in Cangzhou flew to the breeding sites in Mongolia, while another rescued Bustard migrated to the breeding grounds near MAS in Inner Mongolia (Fig. 1). Winter ground fidelity was only observed at a regional scale for Asian Great Bustard, and winter home ranges occupied a series of locations across 30–95 km (Kessler et al. 2013). Compared with the nominal subspecies, Asian Great Bustards are highly mobile even within the migration season, and move between different feeding sites in winter.

How a species responds to climate changes depends strongly on its ecological and environmental tolerances (Parmesan 2006). The divergence between *O. tarda tarda* and *O. tarda dybowskii* occurred in the Early Pleistocene between 1.67 and 2.50 million years ago, indicating independent demographical patterns affected by historical vicariant events, that we hypothesize are climate related (Hewitt 2000). Our demographic analysis further suggested a more recent impact of the last glacial maximum. During the last glacial maximum 10,000–30,000 BP, climatic conditions were favorable for the survival of Great Bustards throughout the Iberian Peninsula during the Holocene and Late Pleistocene (Sánchez et al. 2004). As suggested by Horreo et al. (2013), human activities (agricultural and urban development, hunting pressure) likely drove historical population declines of the nominal Great Bustard (Pitra et al. 2000), and our data support the intensification of human factors since the Neolithic (from 5000 BC onwards) as one of the most important factors influencing the current demographic trend of Asian Great Bustards.

Implication for conservation

Our results showed evidence of population admixture of Asian Great Bustards, but some degree of substructure among wintering grounds is detectable. The current low population size of Asian Great Bustards, and their geographic isolation, makes them more vulnerable to stochastic events that may cause local extirpation. The female effective size ranges between 437 and 656, and we estimate a population size for *O. tarda dybowskii* of around 1456–2187 assuming that 30% of the census population is breeding females (Idaghdour et al. 2004). This is concordant with contemporary population size estimates [1500–2200 (Mi et al. 2016)], and supports the critical conservation status of the subspecies. Habitat and breeding ground protection—and at the very least long-term monitoring—are likely needed to ensure long-term subspecies persistence. Changes to, and lack of, wintering grounds will lead to shifts in food availability, thus affecting the Great Bustard migration routes and population dynamics. Therefore, based on precautionary principles, we propose that the Chinese government consider establishing protected areas in Cangzhou, Hebei province, and Weinan, Shaanxi province, which would facilitate the protection and monitoring of wintering Great Bustards.

The population demographic analysis of the Asian Great Bustard in China suggests a continuous decline since 4000 years ago. We hypothesize that this is related to human factors, such as an increase of human population density, agricultural development, poaching pressure and industrial infrastructure. Importantly, genomic data are being generated from non-invasive samples (Russello et al. 2015) opening the door to analytical frameworks that predict demographic and evolutionary responses of natural populations to disturbance (e.g., Shafer et al. 2016) or to the identification of key landscape or habitat features shaping genomic diversity (Benestan et al. 2016). Future efforts to combine genomic data with satellite tracking technology (Shafer et al. 2016) will greatly aid in our understanding of the migratory patterns and population dynamics of the Asian Great Bustard and will provide vital information for its conservation and management.

Acknowledgments We thank all the students, staff and volunteers who helped in the field. Special thanks to Dr. Elen Peres for valuable comments on the data processing. This research was funded by a Natural Science Foundation of China grant (no. 31500303), a National Nonprofit Institute Research Grant from CAFINT (no. CAFINT2015K05) and the Species Salvation Program of the Department of Fauna and Flora and Nature Reserve Management, State Forestry Administration of China (no. Great Bustard 2016). The experiments comply with the current laws of the country in which they were performed.

References

Alonso JC (2010) The world status and population trends of the Great Bustard (*Otis tarda*): 2010 update. Avian Res 1:141–147

Anna P, Gerard B, García MEL, Morales MB, Axel W, Ignasi M, Santi M (2008) Adverse effects of capture and handling Little Bustard. J Wildl Manage 72:315–319

Bandelt HJ, Forster P, Röhl A (1999) Median-joining networks for inferring intraspecific phylogenies. Mol Biol Evol 16:37–48

Benestan L, Ferchaud A, Hohenlohe P, Garner BA, Naylor GJP et al (2016) Conservation genomics of natural and managed

populations: building a conceptual and practical framework. Mol Ecol 25:2967–2977
Bensch S, Grahn M, Müller N, Gay L, Akesson S (2009) Genetic, morphological, and feather isotope variation of migratory Willow Warblers show gradual divergence in a ring. Mol Ecol 18:3087–3096
BirdLife International (2001) Threatened birds of Asia. The BirdLife International Red Data book. BirdLife International, Cambridge
BirdLife International (2012) Threatened birds of Asia. The BirdLife International Red Data book. BirdLife International, Cambridge
Bohonak AJ (2002) IBD (isolation by distance): a program for analyses of isolation by distance. J Hered 93:153–154
Broders O, Osborne T, Wink M (2003) A mtDNA phylogeny of Bustards (family otididae) based on nucleotide sequences of the cytochrome b gene. J Ornithol 144:176–185
Chabot AA, Hobson KA, Van Wilgenburg SL, Mcquat GJ, Lougheed SC (2012) Advances in linking wintering migrant birds to their breeding-ground origins using combined analyses of genetic and stable isotope markers. PLoS One 7:e43627
Clarke KR, Gorley RN (2015) PRIMER version 7: user manual/tutorial. PRIMER-E, Plymouth
Darriba D, Taboada GL, Doallo R, Posada D (2012) jModelTest 2: more models, new heuristics and parallel computing. Nat Methods 9:772–775
Di ZY, Du CJ (2016) Population restoration and hopes for Great Bustard. For Hum 3:110–111
Erixon P, Svennblad B, Britton T, Oxelman B (2003) Reliability of Bayesian posterior probabilities and bootstrap frequencies in phylogenetics. Syst Biol 52:665–673
Excoffier L, Lischer HEL (2010) Arlequin suite version 3.5: a new series of programs to perform population genetics analyses under Linux and Windows. Mol Ecol Resour 10:564–567
Fu YX (1997) Statistical tests of neutrality of mutations against population growth, hitchhiking and background selection. Genetics 147:915–925
Gamauf A, Gjershaug J, Rov N, Kvaloy K, Haring E (2005) Species or subspecies? The dilemma of taxonomic ranking of some South-East Asian Hawk-Eagles (genus *Spizaetus*). Bird Conserv Int 15:99–117
Harpending HC (1994) Signature of ancient population growth in a low-resolution mitochondrial DNA mismatch distribution. Hum Biol 66:591–600
Heled J, Drummond AJ (2008) Bayesian inference of population size history from multiple loci. BMC Evol Biol 8:1–15
Hewitt G (2000) The genetic legacy of the quaternary ice ages. Nature 405:907–913
Holberton RL, Able KP (2011) Differential migration and an endocrine response to stress in wintering Dark-eyed Juncos (*Junco hyemalis*). Proc R Soc B-Biol Sci 267:1889–1896
Horreo JL, Palacín C, Alonso JC, Milá B (2013) A link between historical population decline in the threatened Great Bustard and human expansion in Iberia: evidence from genetic and demographic data. Biol J Linn Soc 110:515–527
Idaghdour YB, Korrida DA, Chbel F (2004) Mitochondrial control region diversity of the Houbara Bustard *Chlamydotis undulata* complex and genetic structure along the Atlantic seaboard of North Africa. Mol Ecol 13:43–54
Jiang JS (2004) The status of resouree and conservation of Great Bustard in China [D]. Northeast Forestry University, Harbin
Kekkonen J, Hanski IK, Jensen H, Väisänen RA, Brommer JE (2011) Increased genetic differentiation in House Sparrows after a strong population decline: from panmixia towards structure in a common bird. Biol Conserv 144:2931–2940
Kessler AE, Batbayar N, Natsagdorj T, Batsuur D, Smith AT (2013) Satellite telemetry reveals long-distance migration in the Asian Great Bustard *Otis tarda dybowskii*. J Avian Biol 85287:311–320
Kraus RHS, Figuerola J, Klug K (2016) No genetic structure in a mixed flock of migratory and non-migratory Mallards. J Ornithol 157:919–922
Lee JW, Simeoni M, Burke T, Hatchwell BJ (2010) The consequences of winter flock demography for genetic structure and inbreeding risk in Vinous-throated Parrotbills, *Paradoxornis webbianus*. Heredity 104:472–481
Li XM, Liu XC, Zhou JY, Cheng WJ, Yi GL, Wu BX (2005) The survey of the Great Bustard in winter in Tumuji, Inner Mongolia, China. Chin J Zool 40:46–49
Librado P, Rozas J (2009) DnaSP verison 5: a software for comprehensive analysis of DNA polymorphism data. Bioinformatics 25:1451–1452
Liu Z (2006) Genetic diversity of Asian Great Bustard (*Otis tarda dybowskii*) [D]. Northeast Forestry University, Harbin
Liu Y, Keller I, Heckel G (2012) Breeding site fidelity and winter admixture in a long-distance migrant, the Tufted Duck (*Aythya fuligula*). Heredity 109:108–116
Lundberg P (2013) On the evolutionary stability of partial migration. J Theor Biol 321:36–39
Maclean I, Austin GE, Rehfisch MM (2006) Are responses to climate change temperature dependent? Population changes in overwintering migratory shorebirds. J Ornithol 147:26
Mi C, Falk H, Guo Y (2016) Climate envelope predictions indicate an enlarged suitable wintering distribution for Great Bustards (*Otis tarda dybowskii*) in China for the 21st century. PeerJ 4:1–14
Palacín C, Alonso JC (2008) An updated estimate of the world status and population trends of the Great Bustard *Otis tarda*. Ardeola 55:13–25
Parmesan C (2006) Ecological and evolutionary responses to recent climate change. Annu Rev Ecol Evol Syst 37:275–290
Piper WH (2011) Making habitat selection more "familiar": a review. Behav Ecol Sociobiol 65:1329–1351
Pitra C, Lieckfeldt D, Alonso JC (2000) Population subdivision in Europe's Great Bustard inferred from mitochondrial and nuclear DNA sequence variation. Mol Ecol 9:1165–1170
Pitra C, Suárez-Seoane S, Martín CA, Streich WJ, Alonso JC (2011) Linking habitat quality with genetic diversity: a lesson from Great Bustards in Spain. Eur J Wildl Res 57:411–419
Qiao GF, Yu GH, Sun XW, Zou CL, Wang B (2008) Observation and research on wintering habits of *Otis tarda*. Jilin For Sci Technol 37:28–30
Rambaut A, Suchard MA, Xie D (2014) Tracer version 1.6. http://beast.bio.ed.ac.uk/Tracer. Accessed June 2014
Rice WR (1989) Analysing tables of statistical tests. Evolution 43:223–225
Rogers AR, Harpending H (1992) Population growth makes waves in the distribution of pairwise genetic differences. Mol Biol Evol 9:552–569
Rolshausen G, Segelbacher G, Hermes C, Hobson KA, Schaefer HM (2013) Individual differences in migratory behavior shape population genetic structure and microhabitat choice in sympatric blackcaps (*Sylvia atricapilla*). Ecol Evol 3:4278–4289
Ronquist F, Huelsenbeck JP (2003) MrBayes 3: Bayesian phylogenetic inference under mixed models. Bioinformatics 19:1572–1574
Russello MA, Waterhouse MD, Etter PD, Johnson EA (2015) From promise to practice: pairing non-invasive sampling with genomics in conservation. PeerJ 3:e1106
Sánchez E, Gallardo C, Gaertner MA, Arribas A, Castro M (2004) Future climate extreme events in the Mediterranean simulated by a regional climate model: a first approach. Glob Planet Change 44:163–180

Shafer AB, Northrup JM, Wikelski M, Wittemyer G, Wolf JBW (2016) Forecasting ecological genomics: high-tech animal instrumentation meets high-throughput sequencing. PLoS Biol 14:e1002350

State Forestry Administration (2001) The first national terrestrial wildlife survey. China Forestry, Beijing

State Forestry Administration (2016) The second national terrestrial wildlife survey. Beijing **(unpublished)**

Studds CE, Marra PP (2005) Nonbreeding habitat occupancy and population processes: an upgrade experiment with a migratory bird. Ecology 86:2380–2385

Swofford DL (2003) PAUP*. Phylogenetic analysis using parsimony (* and other methods). Version 4.0b10. Sinauer Associates, Sunderland, MA

Tajima F (1989) Statistical method for testing the neutral mutation hypothesis by DNA polymorphism. Genetics 123:585–595

Tamura KNM, Nei M (1993) Estimation of the number of nucleotide substitutions in the control region of mtDNA in humans and chimpanzees. Mol Biol Evol 10:512–526

Tamura K, Peterson D, Peterson N, Stecher G, Nei M, Kumar S (2011) MEGA5: molecular evolutionary genetics analysis using maximum likelihood, evolutionary distance, and maximum parsimony methods. Mol Biol Evol 28:2731–2739

Torstrom SM, Pangle KL, Swanson BJ (2014) Shedding subspecies: the influence of genetics on reptile subspecies taxonomy. Mol Phylogenet Evol 76:134–143

van Wijk RE, Bauer S, Schaub M (2016) Repeatability of individual migration routes, wintering sites, and timing in a long-distance migrant bird. Ecol Evol 6:8679–8685

von Rönn JAC, Shafer A, Wolf JBW (2016) Disruptive selection without genome-wide evolution across a migratory divide. Mol Ecol 25:2529–2541

Weatherhead PJ, Forbes MRL (1994) Natal philopatry in passerine birds: genetic or ecological influences? Behav Ecol 5:426–433

Wilson AG, Arcese P, Chan YL, Patten MA (2011) Micro-spatial genetic structure in Song Sparrows (*Melospiza melodia*). Conserv Genet 12:213–222

Yu CJ (2015) The status and conservation strategies of Asian Great Bustard in Tumuji Nature Reserve, Inner Mongolia. http://www.tmjbhq.com/show-17-245-1.html. Accessed Dec 2015